Desalination and Water Treatment
www.deswater.com

doi:10.5004/dwt.2019.24165

159 (2019) 232–249
August

Techno-economic analysis of combined gas turbine, MED and RO desalination systems to produce electricity and drinkable water

Alireza Javadpour[a], Ebrahim Jahanshahi Javaran[b,*], Khosro Lari[c], Ighball Baniasad Askari[d]

[a]*Faculty of Mechanical and Material Engineering, Graduate University of Advanced Technology, Kerman, Iran, email: alireza.javadpour64@gmail.com (A. Javadpour)*
[b]*Department of Energy, Institute of Science and High Technology and Environmental Sciences, Graduate University of Advanced Technology, Kerman, Iran, email: e.jahanshahi@kgut.ac.ir (E. Jahanshahi Javaran)*
[c]*Faculty of Mechanical and Material Engineering, Graduate University of Advanced Technology, Kerman, Iran, email: k.lari@kgut.ac.ir (K. Lari)*
[d]*Department of Mechanical Engineering, Faculty of Engineering, University of Zabol, Sistan and Baluchestan, Iran, email: eghball.baniasad@uoz.ac.ir (I. Baniasad Askari)*

Received 1 October 2018; Accepted 22 March 2019

ABSTRACT

Water and power cogeneration systems have been received more attention in recent years. In the present research, in addition to techno-economic investigation of the integration of multiple effect desalination/thermal vapor compression (MED/TVC) system and reverse osmosis (RO) system into the gas turbine (GT) power cycle, the GT/MED-TVC/RO configuration is also proposed. At first, the models used for GT, MED-TVC and RO systems are validated with the experimental data in the literature and good correspondence is found. In this study, the effect of air temperature on the GT stack outlet gases and the effect of seawater temperature on the MED-TVC GOR are investigated. Moreover, using the RO energy analysis, the most suitable RO membrane is selected by considering the permeate quality and membrane price. Then, the LCOE and LCOW for three scenarios of GT/MED-TVC with 5000 m^3/d, GT/RO with 5000 m^3/d, and GT/MED-TVC/RO with MED-TVC and RO water production rates of 2000 m^3/d and 3000 m^3/d, respectively are determined. The results of the economic analysis in three scenarios showed that the least electricity cost and the least freshwater production cost belong to GT/MED-TVC and GT/RO configurations, respectively. Furthermore, the effect of number of stages of the MED-TVC system on the energy and economy of the GT/MED-TVC/RO configuration is explored. It was observed that increasing the number of effects from 4 to 7 has no tangible effect on the LCOE. In addition, the output temperature and concentration of GT/MED-TVC/RO plant at different number of MED-TVC effects is determined. Finally, the effect of fuel cost and desalination system scale on the LCOW and LCOE at three configurations are investigated.

Keywords: Multiple effect distillation; Gas turbine; Reverse osmosis; Energy; Economics

1. Introduction

Approximately 97.5% of the water on our planet is located in the oceans and therefore is classified as seawater [1]. Of the 2.5% of the planet's freshwater, approximately 70% is in the form of polar ice and snow and 30% is groundwater, river and lake water, and air moisture [1]. So even though the volume of the earth's water is vast, less than 35 million km^3 of the 1386 million km^3 of water on the planet is of low salinity and is suitable for use after applying conventional water treatment only [1]. According to these interpretations, it seems that the freshwater crisis is one of the greatest problems facing contemporary humans. According to the conducted studies by the International Water Man-

*Corresponding author.

agement Institute, in 1950, twelve countries with a population of about 20 million people were faced with a shortage of water [2]. In 1990, it reached 26 countries with a population of about 300 million and around ten years later, it is expected that 65 countries with a population of about 7 billion will encounter scarcity of water [2]. The energy crisis besides water crisis is also one of the upcoming challenges in the last century that requires high-efficiency systems. Hence, the investigation of water and power generation systems has received considerable attentions in recent years. In these systems, the exhaust heat from GTs or other power cycles is used as the thermal source for thermal desalination systems. This causes recovery enhancement and fuel consumption reduction for cogeneration system. Also, it is possible to combine thermal and membrane desalination systems to produce more drinkable water.

In 2011, Gomar et al. [3] have done widespread research on techno-economic analysis of various types of desalination systems in Asalouyeh.

Many types of research have been done on the simulation of combined power and water production systems. In 2013, the combination of Concentrating Solar Power plants (CSP) with MED & RO desalination systems were investigated by Iaquaniello et al. [4]. They examined economic analysis including some criteria such as power availability, water production rates and environmental benefits. They concluded that if the combined system applied, the water production cost decreases by about 8.8%. The combination of MED-RO desalination units with fossil fuel based utility steam network was investigated by Khoshgoftar-Manesh et al. [5]. The total site analysis and an exergo-economic optimization were applied to find the optimal coupling of site utility and MED-RO desalination system. Loutatidou et al. presented an elementary techno-economic analysis of RO and MED using low enthalpy geothermal energy [6]. They conducted the geothermal MED desalination, driven by direct utilization of geothermal heat, and geothermal RO powered by a geothermal binary power plant. They concluded that the geothermal RO could potentially be a very cost-effective option for seawater geothermal desalination in the Gulf Cooperation Council (GCC) countries. Mahbub et al. presented the combined water and power plant (CWPP) concept to use the power plant at the rated conditions for the most of the time [7]. They analyzed a combined cycle power plant with MSF, MED, RO, MSF-RO hybrid or MED-RO hybrid configurations. They found that the production cost and specific energy consumption of the MED/RO were lower than the MSF/RO. The conceptual design of two new fuel cell-desalination systems (FC/RO and FC/MED) were evaluated by Al-Hallaj et al. [8]. They found that the energy requirement for desalination system is reduced by 8% if the RO input water would be preheated by using the output gas from FC. According to the results of that study, by adding the FC to the desalination systems, the FC waste heat could be used in thermal desalination system and its electricity might be used in RO system to produce fresh water. Ansari et al. [9] utilized three optimization scenarios to optimize dual nuclear power and desalination system. Thermodynamic modeling was performed based on the energy and exergy analysis, while the total revenue requirement (TRR) method was used for economic analysis and the genetic algorithm (GA) was applied for thermo-economic optimization.

Multi-objective optimization of MED/TVC-RO hybrid desalination systems based on the irreversibility concept were performed by Sadri et al. [10]. Following the mathematical modeling via applying energy and concentration conservation laws, the exergy destruction (chemical and physical exergy), exergetic efficiency and system performance were assessed. The final goal of the optimization was the determination of the best trade off between the exergetic efficiencies of MED and RO. The optimum design led to the selection of a MED-RO hybrid system with the highest exergetic efficiency.

In a study by Filippini et al. [11] performance analysis of different configurations of hybrid MED/TVC and RO desalination systems were carried out. In the first configuration, the seawater feed is split between the two systems, which operates un-connectedly. In the second configuration, the membrane process is partially or fully fed with the rejected brine of the thermal process, while in the third configuration the thermal process is partially or fully fed with the rejected brine of the membrane process. These configurations were compared based on the performance indicators including energy consumption, the fresh water productivity, fresh water purity, and recovery ratio. Results showed that placing the RO membrane process upstream in the hybrid system generates the overall best configuration in terms of the quantity and quality of produced fresh water. In a recent study by Al-Obaidi et al. [12], an economic assessment and optimization of the best mentioned configuration [11] of the hybrid desalination systems were explored. Using the economic model, the variation of the overall fresh water cost with operating conditions, namely steam temperature and steam flow rate for the MED/TVC system and inlet pressure and flow rate of the RO system were investigated.

In Iran, RO is the major desalination unit. The only GT/MED-TVC power plant of Iran is located in Qeshm Island which is capable of delivering 18000 m^3 of fresh water per day [13]. In some combined water and power plants (CWP) in the world like Gheshm CWP, despite reducing the produced fresh water temperature by the condenser after the last effect, as well as directing the fresh water to the storage tank, the temperature of the delivered fresh water to the users is not suitable for drinking which may be due to the high ambient temperature of the plant location. On the other hand, the RO permeate has high concentration, whereas the produced fresh water by MED/TVC is nearly salt free and according to the international standards of the World Health Organization (WHO), salinity of good quality drinking water should be below 300 ppm [14]. The combination of RO and MED/TVC unit is one of the alternatives that is suitable to decrease the temperature of produced fresh water that is delivered to the users because of the low output temperature of permeate that is extracted from the RO unit (nearly 25). Moreover, the combination of RO and MED/TVC units is suitable to decrease the TDS of the RO permeate by mixing up with fresh water produced by MED/TVC. Hence, in this study, the hybrid GT/MED-TVC/RO configuration is proposed to produce simultaneously power and drinkable water with suitable quality and at reasonable cost. In fact, in GT/MED-TVC/RO configuration by mixing the desalinated water (with higher concentration and lower temperature) produced by GT/RO

configuration with the one (with lower concentration and higher temperature) by GT/MED-TVC configuration, in addition to have suitable combined temperature, the usage of additives to the permeate is eliminated or minimized in post treatment process of MED/TVC. The cost of additives is a considerable cost in the MED-TVC system. This makes a drinkable water with suitable temperature and TDS at reasonable cost to the users. The net outcome of the above literature review showed that a comprehensive techno-economic analysis of the hybrid GT/MED-TVC/RO system and its comparison with two CWP configurations, namely GT/MED and GT/RO to determine the water production costs and levelized cost of electricity for these three configurations has not yet been fully investigated, an issue which is studied in the present work.

2. Methodology

In this study, three different CWP configurations (GT/MED-TVC, GT/RO and GT/MED-TVC/RO) with the net electricity generation and total water production rates of 12 MW and 5000 m^3/d, respectively are investigated. The process flow diagrams of these configurations are schematically depicted in Figs. 1-3. In the GT/MED-TVC shown in Fig. 1, the exhaust flue gases from the gas tur-

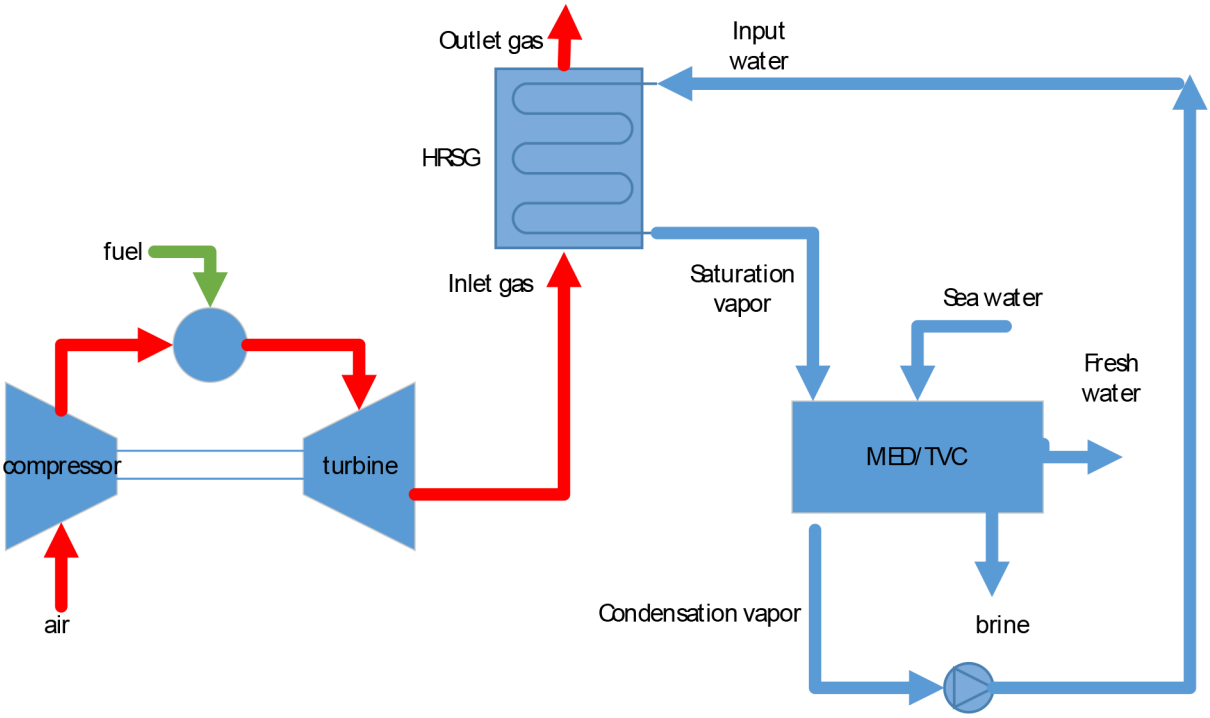

Fig. 1. Schematic of GT/MED-TVC configuration.

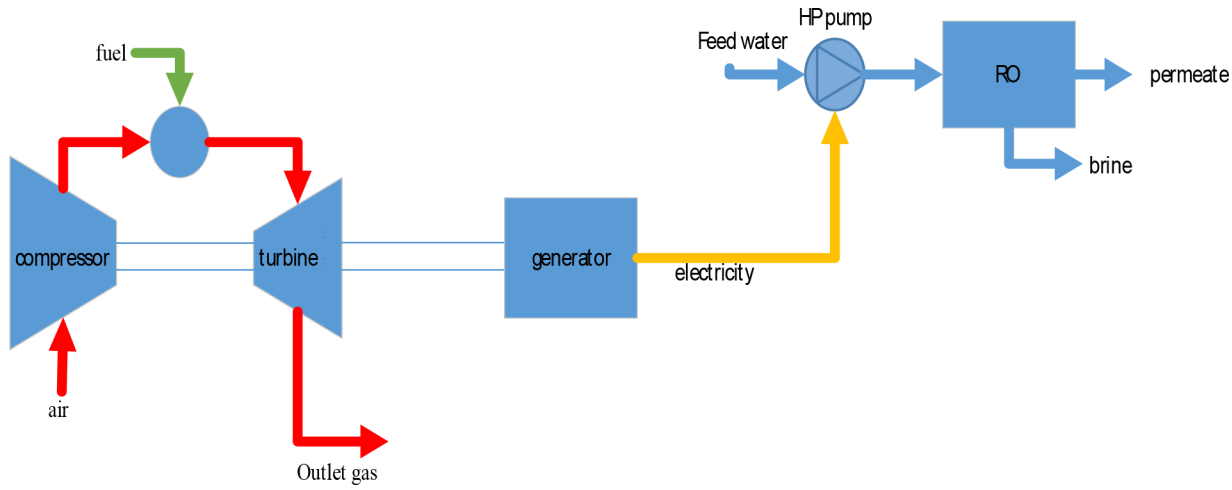

Fig. 2. Schematic of GT/RO configuration.

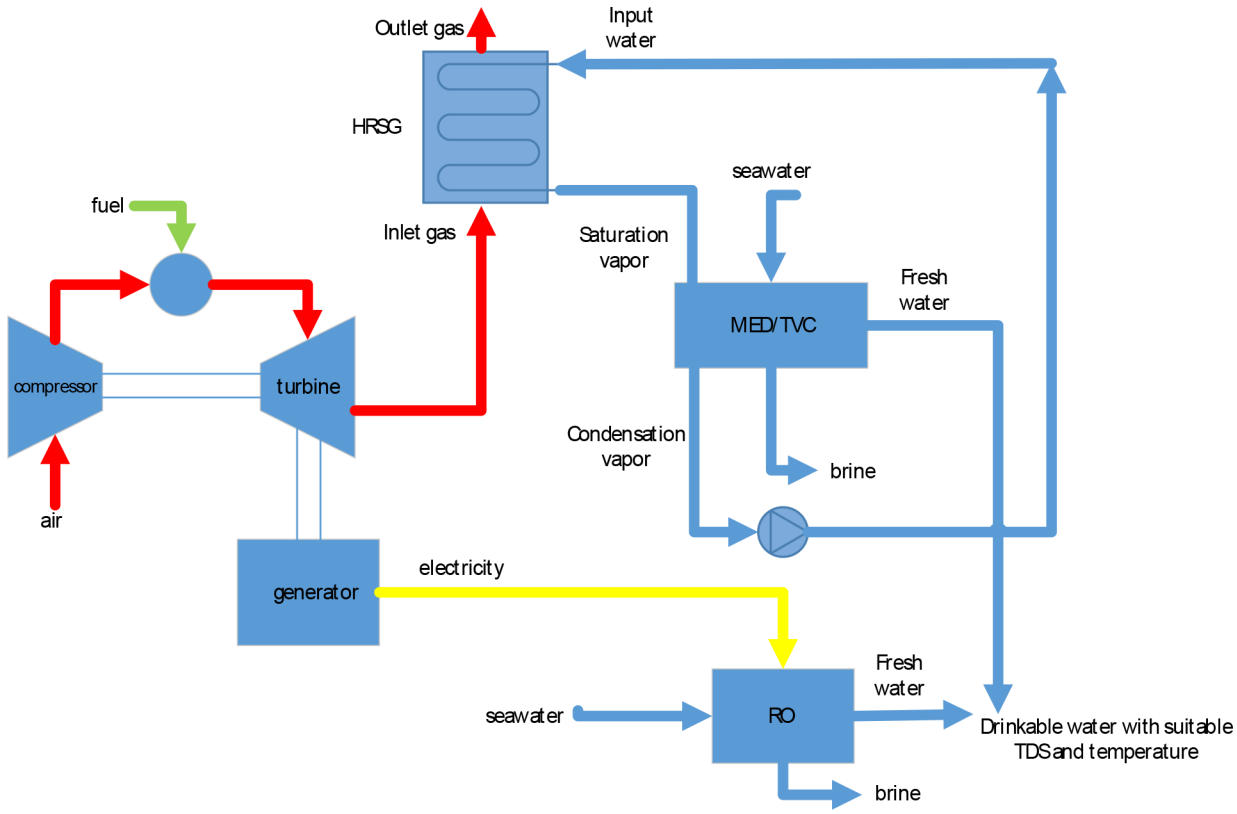

Fig. 3. Schematic of GT/MED-TVC/RO configuration.

bine cycle flow through the heat recovery steam generator (HRSG) shell and provide vapor which is directed to the first effect of the MED-TVC desalination unit. Seawater sprays on the MED-TVC tube bundles of each effect and evaporates. The steam generated in the first effect flows to the next effect and the same phenomenon taken place at subsequent effects. Desalinated water produced in each effect, is collected as distillate. For the GT/RO plant as shown in Fig. 2, the net generated electricity from GT cycle provides the required energy for the RO pump such that the feed water could be passed through the membranes of the RO unit and made fresh water. In the GT/MED-TVC/RO configuration shown in Fig. 3, the waste heat of the GT stack and the net generated electricity from GT cycle are utilized to run the MED-TVC and RO desalination systems. It should be noted that at three mentioned configurations, the GT cycle should produce the required electricity of desalination systems in addition to the net electricity generation rate of 12 MW which should be delivered to the user. Moreover, as it is seen in Fig. 3, the produced fresh water by the MED-TVC and RO desalination systems are blended together to make a drinkable water with suitable TDS and temperature.

To achieve the techno-economic analysis of the hybrid GT/MED-TVC/RO system and its comparison with two CWP configurations, namely GT/MED-TVC and GT/RO, after thermodynamic modeling of the GT cycle including the air compressor, the combustion chamber and the gas turbine at section 2.1.1, the HRSG modeling is provided at section 2.1.2. Sections 2.1.3 and 2.1.4 are devoted to the modeling of MED-TVC and RO desalination systems, respectively. Finally, the levelized cost of electricity and water, payback period as well as the desired techno-economic comparison are made by the aid of materials presented at section 2.3. To achieve the objective mentioned above, MATLAB and EES codes based on the solution strategy presented in section 2.4 are developed.

2.1. Modeling

2.1.1. Gas turbine cycle

To find outlet temperature and gas flow rate of the gas turbine, a simulation program was developed in EES software. In this section, modeling of different parts of the gas turbine cycle is carried out.

2.1.1.1. Air compressor

Air is entering the compressor at the ambient pressure (1 bar) and temperature (T_1). The compressor outlet temperature (T_2) is a function of compressor pressure ratio (r_{Ac}), compressor isentropic efficiency (η_{AC}) and specific heat ratio (k_a) as follows:

$$T_2 = T_1 \times \left(1 + \frac{1}{\eta_{AC}}\left(r_{AC}^{\frac{k_a-1}{k_a}} - 1\right)\right) \quad (1)$$

The compressor power and specific heat at constant pressure can be expressed as [15]:

$$\dot{W}_{AC} = \dot{m}_a C_{pa}\left(T_2 - T_1\right) \tag{2}$$

$$C_{pa}(T) = 1.048 - \left(\frac{3.83T}{10^4}\right) + \left(\frac{9.45T^2}{10^7}\right) - \left(\frac{5.49T^3}{10^{10}}\right) + \left(\frac{7.92T^4}{10^{14}}\right) \tag{3}$$

2.1.1.2. Combustion chamber

Energy balance equation for combustion chamber which is a function of air mass flow rate, fuel lower heating value (LHV) and combustion efficiency (η_{cc}) is as follows:

$$\dot{m}_a h_2 + \dot{m}_f LHV = \dot{m}_g h_3 + \left(1 - \eta_{cc}\right)\dot{m}_f LHV \tag{4}$$

Because of pressure drop across the combustion chamber, the combustion chamber outlet pressure is described by:

$$\frac{P_3}{P_2} = \left(1 - \Delta P_{cc}\right) \tag{5}$$

where ΔP_{cc} is the pressure loss across the combustion chamber. The combustion equation of the natural gas fuel with 90% of CO_2 and its species coefficients can be expressed as follows:

$$CH_4 + 2\times Y\left(O_2 + 3.76N_2\right) \rightarrow pCO_2 + \left(1-p\right)CO + 2H_2O + 2\times Y\times 3.76N_2 + \left[2Y - p - \left(\frac{1-p}{2}\right) - 1\right]O_2 \tag{6}$$

$$n_{CO_2} = p \tag{7}$$

$$n_{CO} = 1 - p \tag{8}$$

$$n_{H_2O} = 2 \tag{9}$$

$$n_{N_2} = 2\times Y\times 3.76 \tag{10}$$

$$n_{O_2} = 2Y - p - \left(\frac{1-p}{2}\right) - 1 \tag{11}$$

$$AF = 2Y\times 4.76\times \frac{M_{air}}{M_{CH_4}} \tag{12}$$

$$\dot{m}_a = AF\times \dot{m}_f \tag{13}$$

$$Y = \frac{percent\ of\ theoretical\ air}{100} \tag{14}$$

$$p = \frac{percent\ of\ CO_2}{100} \tag{15}$$

where AF is the molar air to fuel ratio, M_f and M_a are molar mass of the fuel and air, respectively.

2.1.1.3. Gas turbine

The gas turbine outlet temperature (T_4), which is a function of gas turbine isentropic efficiency (η_{GT}), the gas turbine inlet temperature (T_3) and gas turbine pressure ratio ($\frac{P_3}{P_4}$) is presented as follows:

$$T_4 = T_3\left(1 - \eta_{GT}\left(1 - \left(\frac{P_3}{P_4}\right)^{\frac{1-k_g}{k_g}}\right)\right) \tag{16}$$

The GT output power (W_{GT}), GT mass flow rate ($\dot{m}_g$) and the net output power ($\dot{W}_{net}$) are determined as follows:

$$\dot{W}_{GT} = \dot{m}_g C_{pg}\left(T_3 - T_4\right) \tag{17}$$

$$\dot{m}_g = \dot{m}_f + \dot{m}_a \tag{18}$$

$$\dot{W}_{net} = \dot{W}_{GT} - \dot{W}_{AC} \tag{19}$$

where C_{pg} is presented as follows [15]:

$$C_{pg}(T) = 0.991 + \left(\frac{6.997T}{10^5}\right) + \left(\frac{2.712T^2}{10^7}\right) - \left(\frac{1.2244T^3}{10^{10}}\right) \tag{20}$$

2.1.2. Heat recovery steam generator

The Heat Recovery Steam Generator (HRSG) includes an economizer and an evaporator which produces the required motive steam for MED/TVC system.

Because the dry steam is used as the motive steam in the MED/TVC, the super heater section is not needed for the boiler. The HRSG design in the actual technology is based on the concepts of pinch point and approach point, which define the steam and gas temperature profiles. The pinch point temperature difference is the difference between the hot gas temperature at the evaporator exit and drum saturation temperature ($T_{sat@Dram}$), and the approach temperature is the difference between drum inlet water temperature and the saturated temperature. The pinch point and approach point are calculated using Eq. (21), (22) [16]:

$$T_{pin} = T_g - T_{sat@Drumpressure} \tag{21}$$

$$T_{app} = T_{sat@Drumpressure} - T_2 \tag{22}$$

The energy and mass balance equations for the economizer and evaporator are demonstrated as follows:

Evaporator:

$$M_m h_{fg} = m_g Cp_g\left(T_{g\ in} - T_g\right) \tag{23}$$

Economizer:

$$M_m Cp_l\left(T_2 - T_1\right) = m_g Cp_g\left(T_g - T_{g,out}\right) \tag{24}$$

For designing the HRSG system, it is essential to calculate the heat transfer areas which can be obtained by [17]:

$$A = \frac{\dot{Q}}{U\Delta T_{LMTD}} \tag{25}$$

where, Q and ΔT_{LMTD} are heat flow rate and logarithmic temperature difference.

Logarithmic mean temperature difference and overall heat transfer coefficient can be determined as follows:

$$\Delta T_{LMTD} = F_T \times \frac{\Delta T_{\max} - \Delta T_{\min}}{\ln\left(\frac{\Delta T_{\max}}{\Delta T_{\min}}\right)} \tag{26}$$

$$\frac{1}{U} = \frac{1}{\eta_o h_o} + f_o + \frac{A_t}{A_{wi}} f_i + \frac{A_t}{A_{wi}} \frac{1}{h_i} + \frac{A_t}{A_w} \frac{d_o \ln\left(\frac{d_o}{d_i}\right)}{2K_m} \tag{27}$$

where, F_T is a coefficient representing the angle of incidence between gas flow and pipes [18].

In this research, "U" was assumed to be in the range of 20–50 (W/m²·K) for economizer and in the range of 70–110 (W/m²·K) for evaporator. Therefore, U was considered as the average value of this ranges that is 35 (W/m²·K) for economizer and 90 (W/m²·K) for evaporator [18].

2.1.3. MED/TVC desalination system

The parallel-cross feed MED/TVC plant includes condenser, flashing boxes, thermal vapor compression and evaporators.

- To perform the thermodynamic modeling of the MED/TVC system, the following assumptions are considered:
  - The plant is operated at steady-state condition.
  - Temperature difference in each effect is assumed to be the same.
  - The distillate is salt free.
  - The flow rate of all effects is the same.
  - Heat losses from all the components of the MED/TVC are negligible.
  - The salinity of first effect brine is 70000 ppm.

In the present study, the actual data of the Tripoli plant, located in Italy were used [17] to validate the accuracy of the results. In order to determine the thermal performance ratio, heat transfer area and flow rate of produced water, three groups of equations were solved; a) the mass, energy and salinity balance equations [Eqs. (31)–(35), Table 1], b) the required heat transfer area for each effect and condenser [Eqs. (36)–(39), Table 1].

The ratio of motive steam to entrained vapor (M_m/M_{ev}) is the most essential part in modeling the MED/TVC desalination system. This ratio is a function of motive steam pressure (P_m), compressed vapors pressure (P_s) and the pressure of entrained vapor (P_{ev}), as follows:

The semi-empirical method developed by reference [20] is applied to calculate entrainment ratio that is given as follows:

$$R_a = 0.235 \times \frac{P_s^{1.19}}{P_{ev}^{1.04}} \times Er^{0.015} \tag{30}$$

Table 1
MED/TVC equations [19,20]

Equations	Descriptions	
$D_1 \cdot \lambda_1 = \left(M_m + M_{ev}\right) \cdot \lambda_s - F_1 \cdot C_p \cdot \left(T_1 - T_f\right)$	Energy balance of effect 1	(31)
$D_i \cdot \lambda_i = \left(D_{i-1} \cdot \lambda_{i-1} + d_{i-1} \cdot \lambda_{i-1} + d'_{i-1} \cdot \lambda'_{i-1}\right) - F_i \cdot C_p \cdot \left(T_i - T_f\right) + B_{i-1} \cdot C_p \cdot \left(T_{i-1} - T_i\right)$	Energy balances of effect 2 to n	(32)
$d_i = \frac{\boldsymbol{B}_{i-1} \times C_p \times \left(T_{i-1} - T'_i\right)}{\lambda_i}$	Mass flow rate of vapor flashed off from the brine	(33)
$d'_i = D_{i-1} \times C_p \times \frac{T_{c_{i-1}} - T''_i}{\lambda'_i}$	Mass flow rate of vapor formed in the flash box	(34)
$GOR = \frac{D_{total}}{M_m}$	Gain output ratio	(35)
$A_1 = \frac{M_s \cdot \lambda_s}{U_1 \cdot \left(T_s - T_1\right)}$	Heat transfer area of effect 1	(36)
$A_i = \frac{\left(D_{i-1} + d_{i-1}\right) \cdot \lambda_{i-1} + d'_{i-1} \cdot \lambda'_{i-1}}{U_i \cdot \left(T_{v_{i-1}} - T_i\right)}$	Heat transfer area of effect 2 to n	(37)
$A_{tot} = \sum_{i=1}^{n} A_i$	Total heat transfer area of effects	(38)
$A_c = \frac{M_c \cdot \lambda_n}{U_c \cdot \left(LMTD\right)_c}$	Heat transfer area of condenser	(39)

2.1.4. RO desalination system

The RO system was designed for full load operation (24 h/d) and 40% recovery. The feed water is preheated physically and chemically and then it is pumped to the RO membranes configured in standard pressure vessels (6 membranes per pressure vessel) [21]. Also, the most designed system with 40–45% recovery ratio has the same configuration. The total number of membranes needed was calculated by changing feed water flow rate to reach the adequate recovery ratio of 40–45% and the permeate water with acceptable quality of 300–600 ppm). The design assumptions of the RO system are summarized in Table 2.

The high pressure pumps consume almost 74% of total energy consumption in RO system. The rest is divided according to the energy cost breakdown for a Sea Water Reverse Osmosis (SWRO) desalination plant, as given in [22]. ROSA software, which is developed by DOW chemical company [22], was used to calculate the energy consumption of the high pressure pumps by applying the Persian Gulf's seawater salinity and temperature for the specific recovery ratios. Assuming high pressure pump efficiency is 90%, the specific energy consumption of the plants was assumed to be 4.2 kWh/m^3.

2.2. Economic analysis

Two desalination plants (MED and RO) were assumed to be powered by a gas turbine with 24 h full load operation and 12 MWh capacity. Both desalination plants are assumed to be located at seashore (approximately 1 km of the shore) and the intake water to these systems is a composition of Persian Gulf seawater (30 and 46000 ppm). The economic analysis of the dual purpose system (electricity/water) includes all the costs over its lifetime such as the capital direct costs (DC) and indirect costs (IC), the operation and maintenance cost (O&M), and the fuel costs. The levelized cost of energy (LCOE), and levelized cost of water (LCOW) definitions were used to determine the unit costs of electricity and water. The LCOE and LCOW are the unit prices of the electricity and water over the lifetime of the project, respectively. The capital recovery factor (CRF) was used to convert the direct and indirect cost to annualized form over the life time (n) of a project:

$$CRF(i,n)=\frac{i\cdot(1+i)^n}{(1+i)^n-1} \tag{31}$$

where "i" is the annual real interest rate and the life time of the project were considered as 2.56% and 25 years, respectively [23]. The annualized costs were achieved by multiplying the CRF by capital costs of the system as follows:

$$C_{CAPEX}=C\times CRF(i,n) \tag{32}$$

Applying the direct and indirect costs, the CRF, the operation and maintenance costs and the amount of fresh water production and electricity generation over a year, the LCOE ($/kWh) and LCOW ($/m^3) of the system were calculated using the following equation [11]:

$$LCOE=\frac{C_{CAPEX}(D)+C_{CAPEX}(ID)+C_{SP}+C_{Ins}+C_L+C_f}{AEG} \tag{33}$$

$$LCOW=\frac{\begin{array}{l}C_{CAPEX}(D)+C_{CAPEX}(ID)+C_{SP}+C_{Ins}\\+C_L+C_{MEM(RO)}+C_{el(MED)}+C_{el(RO)}\end{array}}{AWP} \tag{34}$$

where $C_{CAPEX}(D)$, $C_{CAPEX}(ID)$ are total direct and indirect capital expenditure of the desalination plant, respectively (USD $/y), AWP: annual fresh water production (m^3/y), AEG: annual energy generation (kWh/y), C_{Ins}: cost of insurance (USD $/y), C_{sp}: cost of spare part's replacement (USD $/y), C_L: cost of labor (USD $/y), $C_{MEM(RO)}$: cost of membrane replacement (USD $/y), C_f: cost of fuel ($/y), $C_{el(MED)}$, $C_{el(RO)}$ are electricity costs of MED and RO, respectively. The electricity consumption of MED and RO units were considered to be 1.55 kWh/m^3 and 4.2 kWh/m^3, respectively [24]. The specific cost of labor for MED is the double of RO according to [25]. The direct RO costs were considered to be 900 ($/m^3/d) that was used for RO plants in Persian Gulf [24]. The instrument includes air compressor, combustion chamber, gas turbine, heat recovery and steam generator, pump, MED/TVC and RO system. The direct cost of the CHP and HRSG systems are shown in Table 3 and the direct cost of the MED/TVC system is presented in Table 4. Also, the assumptions applied in the indirect and operation costs of the systems are summarized in Table 5

SPB (simple payback time) was chosen as the main objective function for the techno-economic analysis. SPB is stated as the period of time needed to achieve the break-even point:

$$SPB=\frac{Z_{total}+Z_{operation}}{R_{el}+R_{fresh}} \tag{35}$$

$$\begin{array}{l}Z_{total}(DC+INDC)=Z_{\text{turb}}+Z_{\text{generator}}+Z_{\text{combustion}}+\\Z_{\text{compressor}}+Z_{\text{HRSG}}+Z_{MED-TVC}+Z_{RO}\end{array} \tag{36}$$

where, R_{el} and R_{fresh} are the revenue of the plant deriving from the electricity production and the revenue related to the sale of desalinated water, respectively.

Table 2
Input data and assumptions used in the design of the RO plant

Parameter	Value
Operation time per day	24 h
Number of passes	1
Water recovery per pass	40%
Efficiency of RO	
Pump efficiency	0.9
Flow factor	0.85
RO membrane features	
Membrane type	SW30XHR-400i
Active surface	37.16 m^2
Element diameter	7.87 in
Maximum operation pressure	83 bar
Minimum salt rejection	99.6 %
Number of elements per pressure vessel	6

Table 3
Capital cost of the gas turbine cycle and HRSG systems

Instrument	Capital cost of instrument	Reference
Gas turbine	$Z_{turb} = \dot{W}_{turb}\left(1318.5 - 98.328\ln\left(\dot{W}_{turb}\right)\right)$	[23]
HRSG	$Z_{HRSG} = 8500 + 409\left(A_{HRSG}\right)^{0.85}$	[23]
Air compressor	$Z_{AC} = \frac{39.5\dot{m}_a}{0.9 - \eta_{AC}}\left(\frac{P_{dc}}{P_{suc}}\right)\ln\left(\frac{P_{dc}}{P_{suc}}\right)$	[26]
Combustion chamber	$Z_{cc} = \left(\frac{46.08\dot{m}_a}{0.995 - \frac{P_9}{P_7}}\right)\left[1 + \exp(0.018T_9 - 26.4)\right]$	[23]
Generator	$Z_{generator} = 60\left(W_{turbine} - W_{compressor}\right)^{0.95}$	[23]

Table 4
Direct costs of MED/TVC desalination unit with capacity of 5000 m^3/day [10]

Main investment ($/m^3/day)	1700
Post-treatment plant ($/m^3/day)	120
Open sea water intakes ($/m^3/day)	313
Drinking water storage and pumping ($/m^3/day)	100
Water storage tank ($/m^3/day)	100

Table 5
Indirect and operation costs of the system [10]

Indirect cost (IC)	
Freight & insurance rate during construction	5.00% DC
Owner's cost rate	10.00% of direct material and labor cost
Contingency rate	10.00% of DC
Construction overhead (interest during construction)	12.24% of DC
Operation costs (OC)	
Spare parts replacement	1.5% of total DC
Insurance	0.05% of total DC
Natural Gas auxiliary boiler costs ($/m^3)	0.02
Labor cost of product water ($/m^3)	0.1
Electricity cost	Depend on LCOE

2.3. Solution algorithm

In this study Matlab & EES codes were developed to solve the set of equations. The solution strategy could be briefly described as follows:

1. The GT cycle is simulated by the aid of Eqs. (1)–(20) in EES and the temperature of gases at the stack output is calculated.
2. MED/TVC GOR is calculated with the aid of Table 1 in Matlab.
3. The permeate concentration, flow rate and recovery ratio of RO plant is calculated by ROSA software.
4. The levelized cost of electricity and water as well as payback period are calculated using Eqs. (42)–(44) with the aid of Tables 3–5 in Matlab.

3. Validation

In this section, the models developed for GT, MED-TVC and RO systems are individually validated against those of several previous studies found in the literature.

3.1. Gas turbine

A computer program was developed in EES software for solving the mathematical model of the Gas turbine cycle that is composed of a compressor, a combustion chamber and a turbine. The results were compared with the actual data from a typical GT located at Riyadh [27]. The validation of GT is described in Table 6.

3.2. MED/TVC

For solving the mathematical model of the MED/TVC system, a computer program was developed in MATLAB. The results were compared with the actual data from the Tripoli [19] and Umm Al-Nar [28] desalination plants. Tripoli plant consists of two units of 5000 m^3/d low temperature horizontal tube multi-effect distillation with thermal vapor compressor, each effect includes a condenser and four effects. The Umm Al-Nar (UAN) plant consists of seven multi stage flash (MSF) desalination units and two MED units. The unit capacity of MED plant is 3.5 MIGD

(million imperial gallons per day), and the thermal energy requirement is 85 ton of low-pressure steam per hour [28]. The validation of MED-TVC is described in Table 7.

Table 6
Comparison of the present GT simulation results with the experimental data of GT located at Riyadh

	Designed model	Actual data from GT located at Riyadh
T_1 (°C)	25.4	25.4
P_1 (kPa)	96.4	96.4
T_3 (°C)	1105	1105
r_{AC}	10.83	10.83
$\dot{m}_a(kg/s)$	180	180
$\eta_{AC}(\%)$	84	84
$\eta_{GT}(\%)$	94	94
W_{net} (MW)	59.61	58.1
W_{GT} (MW)	121.48	120.64

3.3. RO

The RO experimental data were collected from an industrial plant with a capacity of 380 m^3/day located in Santorini Island [29]. The plant includes 6 pressure vessels, each one containing six membrane modules. The SW30HR-380 membranes were considered in the present work.

The validation of designed model with the experimental data from an industrial plant were expressed in Table 8 for feed pressures of 62 bar and 57 bar, respectively.

4. Results

4.1. Effect of air temperature on the GT stack outlet gases

The power output ratio of the plants was assumed to be 12 MWh. The temperature of inlet seawater to the condenser of MED plant during the cold seasons (October to March) and warm seasons (April to September) of the year is one of the important design parameters. The average seawater temperature of the Persian Gulf was assumed to be 32°C in the warm seasons and 27°C in the cold seasons. By changing the air temperature during the year, the outlet gas flow rate of the GT stack also changes. Hence, assuming the constant inlet and outlet temperature and mass flow rate of water in

Table 7
Mathematical model comparison of MED/TVC against three commercial plants with same number of effects

	Designed model	Actual data of Tripoli [17]	Designed model	Actual data of Umm plant [25]
Number of effects n	4	4	6	6
Motive pressure P_m (kPa)	2300	2300	2500	2500
Top brine temperature T_1 (°C)	60.1	60.1	61.8	61.8
Minimum brine temperature T_n (°C)	45.4	45.4	42.8	42.8
Feed seawater temperature T_f (°C)	41.5	41.5	40	40
Cooling seawater temperature T_{SW} (°C)	31.5	31.5	30	30
Motive steam flow rate D_m, (kg/s)	8.8	8.8	21.2	21.2
Temperature drop per effect, ΔT (°C)	4.9	4.9	3.8	3.8
Entrainment ratio (Ra)	14.1	14.1	1.36	1.36
Expansion ratio (ER)	240.9	240.9	299.94	299.94
Compression ratio (CR)	2.66	2.66	3.12	3.12
Distillate production D (kg/s)	58.2624	57.8	186.379	184.4
Gain output ratio (GOR)	6.6207	6.51	8.7915	8.6

Table 8
Comparison of the designed model and the experimental data for 62 and 57 bar feed pressure

	Designed model (62 bar)	Experimental data [27] (62 bar)	Designed model (57 bar)	Experimental data [27] (57 bar)
Q_f (m^3/h)	43.58	43.58	43.58	43.58
X_f (mg/l)	42000	42000	42000	42000
T_f (°C)	25	25	25	25
N_{pv}	6	6	6	6
$N_{membrane}$	36	36	36	36
X_p (mg/l)	329.75	380	360.76	395
Q_p (m^3/h)	15.06	15.71	13.03	13.62

the HRSG system, the variation of the air temperature causes changing the outlet gas temperature in the HRSG. In this section, the effect of compressor inlet air temperature on the HRSG outlet gas temperature was investigated for GT/MED and GT/MED-TVC/RO configurations by employing Eqs. (16)–(20). As shown in Fig. 4, by increasing the compressor inlet air temperature, the HRSG outlet gas temperature is increased. Increasing the compressor inlet air temperature causes the outlet gas temperature enhancement for both GT/MED-TVC and GT/MED-TVC/RO systems.

4.2. Effect of seawater temperature on the MED-TVC GOR

One of the parameters that was considered in the current study is the input seawater temperature. Considering the changes in seawater temperature during different seasons of the year, the effect of increasing seawater temperature on the GOR of the system was investigated using the equations shown in Table 1. Fig. 5 shows monthly variation of the input seawater temperature [30,31] and its effect on the GOR of the system. The input data of Tripoli plant [17] that are given in Table 7 are used for calculating GOR, but with 6 effects. As it is shown in this figure, the highest performance ratio belongs to August, and the lowest belongs to February. In fact, the higher seawater temperature entails the higher feed water temperature that is sprayed into the effects, which consequently causes to have the greater GORs in warm months [Eq. (35)].

4.3. RO energy analysis

In order to simulate the reverse osmosis system, the quality of fresh water and the prices of membranes should be considered. For this purpose, the permeate concentration (X_p), the permeate flow rate (Q_p), the recovery ratio and the price of the membranes were calculated for 13 different types of membranes in order to choose the most appropriate one.

As mentioned formerly, this analysis was done with ROSA software which contains six tabs:

1. Project information: Flow, pressure and temperature units are defined in this table. Also, the balance analysis can be done with different kinds of salts, NaCl is chosen in the present analysis.
2. Feed water data: In this tab the feed water characteristics such as temperature, flow rate, water type and total dissolved (TDS) solids soluble in feed water are defined. The TDS was set as 46000 mg/L based on the Persian Gulf seawater salinity.
3. Scaling information: This tab is only activated when in the feed water data tab, the individual solutes specified by user.
4. System configuration: In this tab the main parameters for designing the RO system is specified, this parameters are shown in Table 9. Also, the specific energy consumption of the plant was assumed to be 4.2 kWh/m^3 based on the Persian Gulf seawater salinity [24].
5. Report: After specification of the input parameters, the ROSA report presents the final information such as the system recovery and the flow rate, pressure and TDS of the permeate and brine water.
6. Cost analysis: In this tab the input parameters such as project life, interest rate and element cost should be imported and then ROSA gives the capital and operating costs of the system.

The input requirements for the software are shown in Table 9. Also, the simulation results of the RO system are presented in Table 10.

According to the results of Table 10, the selected membrane was SW30XHR-400i by considering the permeate quality and membrane price.

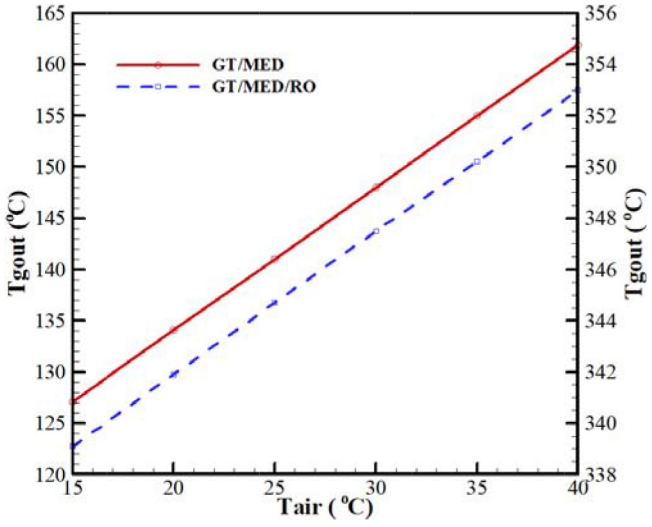

Fig. 4. Effect of the compressor inlet air temperature on the HRSG outlet gas temperature, at GT/MED and GT/MED/RO configurations.

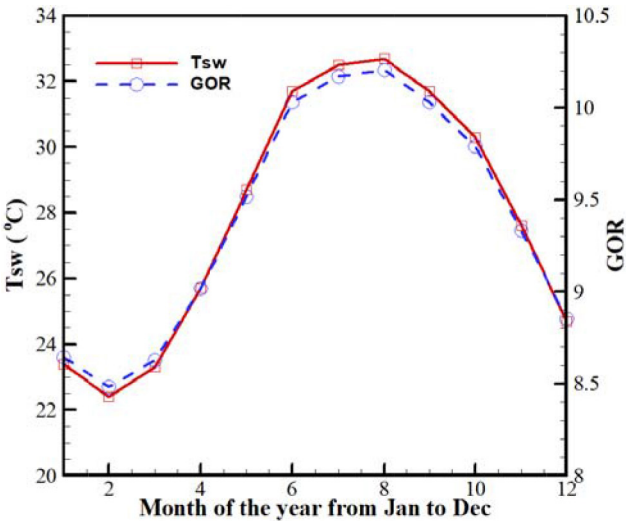

Fig. 5. Monthly variation of the inlet seawater temperature and its effect on the GOR of the system.

4.4. GT/MED-TVC, GT/RO and GT/MED-TVC/RO configurations

The combination of thermal and membrane water distillation technologies is usually considered in the GT or Rankine cycle (RC) power plants. In the RC power plants, the MED unit is replaced by condenser of the cycle, or part of the high pressure steam of the steam turbine is used as the motive steam of the MED/TVC unit. This causes decreasing the RC electrical efficiency. However, in the GT power plant, the waste thermal energy in the stack is used to produce the fresh water in the MED/TVC unit. This technique helps to reduce the water production cost by eliminating the thermal energy cost that is required in desalination process. In this part of the study, three different CWP configurations (GT/MED-TVC, GT/RO and GT/MED-TVC/RO) were investigated. For three configurations of the study, the net electricity generation and total water production rates were assumed to be 12 MW and 5000 m^3/d, respectively. In order to evaluate the unit cost of the fresh water produced by MED-TVC and RO units, three scenarios are considered:

1. GT/MED-TVC with 5000 m^3/d (Fig. 1).
2. GT/RO with 5000 m^3/d (Fig. 2).
3. GT/MED-TVC/RO with MED-TVC and RO water production rates of 2000 m^3/d and 3000 m^3/d, respectively (Fig. 3).

Table 9
Input requirements for the ROSA software

Parameter	Unit	Value
Q_f	M^3/h	43
X_f	ppm	46000
T_f	°C	41.5
P_f	kPa	6200
Number of stages		1
Number of pressure vessels		6
Number of elements per pressure vessels		6

Table 10
Simulation results of the RO system for different types of the membranes

Membrane type	Q_p (m^3/h)	X_p (ppm)	Rec (%)	Price ($/element) [29]
SW30HR-380	13.28	842.98	30.87	988.5
SW30XHR-440i	13.53	554.81	31.47	890
SW30XHR-400i	13.11	515.59	30.49	850
SW30HRLE-440i	14.24	735.32	33.11	738.95
SW30HRLE-400i	13.87	680.92	32.25	758
SW30HRLE-370/34i	13.27	615.34	30.87	780
SW30XLE-440i	14.76	852.14	34.33	850
SW30XLE-400i	14.39	788.75	33.46	820
SW30ULE-440i	15.7	1460.83	36.52	890
SW30ULE-400i	15.34	1352.23	35.68	850
SW30HRLE-4040	5.3	316.82	12.32	459
SW30-4040	6.58	459.07	15.3	399
SW30-2540	1.17	1445.52	2.72	225

4.4.1. The LCOE and LCOW of the plants

The LCOE of all plants were calculated according to Eq. (42) where the capital, direct, indirect and operating costs of the system were calculated based on the cost information shown in Tables 3–5. The gross generated electricity in the GT power plants was assumed to be used for two purposes; one for the users and the other part is assigned to be used in the MED-TVC or RO desalination plants. According to the specific electricity consumptions of RO and MED-TVC units (4.2 kWh/m^3 and 1.55 kWh/m^3, respectively), the electricity needed for the desalination plants to produce 5000 m^3/d of freshwater were calculated as 322 kWh for GT/MED-TVC, 875 kWh for GT/RO and 654 kWh for GT/MED-TVC/RO system. It is worth mentioning that, the gross electricity is sum of the total net electricity (12000 kWh) and the electricity consumption that is consumed by the desalination units. In the present work, two different LCOEs were calculated based on the gross and net electricity generation rates ($(LCOE_{gross}, LCOE_{net}) \cdot LCOE_{gross}$)was used in the calculations to obtain the *LCOW* and $LCOW_{net}$ applied to determine the unit electricity cost that is delivered to users. Fig. 6 shows the for GT/MED-TVC, GT/RO and GT/MED-TVC/RO systems. As shown in Fig. 6, because the electricity consumption of the MED-TVC system (1.55 kWh/m^3) is lower than that of the RO system (4.2 kWh/m^3) the $LCOW_{gross}$ of GT/MED-TVC system is lower than that of GT/RO system. Also, the $LCOW_{gross}$ GT/MED-TVC/RO is higher than the GT/MED-TVC, because of the high electricity consumption of the RO unit.

For three configurations, the LCOW was calculated from Eq. (43). LCOW of the plants were determined by using the

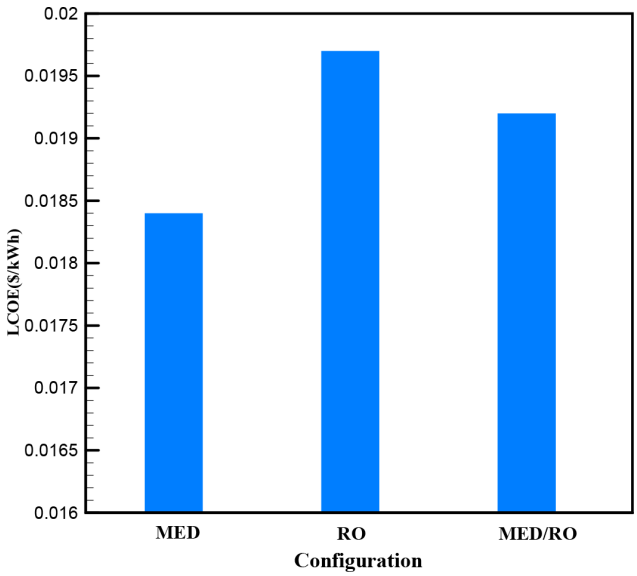

Fig. 6. LCOE of GT/MED-TVC, GT/RO and GT/MED-TVC/RO systems.

$LCOW_{gross}$ of each plant as well as the capital, direct, indirect and operating costs of RO and MED-TVC units shown in Tables 3–5. Fig. 7 shows the LCOW of GT/MED-TVC, GT/RO and GT/MED-TVC/RO systems. As it can be seen from Fig. 7, the LCOW of RO is lower than two other plants. Based on the $LCOW_{gross}$ of each plant (Fig. 6), the portion of electricity cost in LCOW were obtained as 15%, 4% and 10% for RO, MED-TVC and MED-TVC/RO plants, respectively. The most important cost parameter that affects the LCOW of each plant is the main investment desalination units. Because the main investment cost of RO is lower than that of MED, the unit cost of fresh water produced by GT/RO and GT/MED-TVC/RO are lower than that of by GT/MED-TVC configuration.

It is interesting to mention that, the input heat of the MED-TVC system is supplied from the excess heat of a gas turbine that doesn't have any cost for the system. Therefore, if the MED-TVC main investment decreases from \$1700/m³/d to \$1066/m³/d, the LCOW value for both GT/MED-TVC and GT/RO systems are equal. The results may change for the case when the MED-TVC heat source would be costly (fuel boiler, solar thermal, etc).

4.4.2. The effect of number of MED-TVC stages on the GT/MED-TVC/RO configuration

In this section, the effect of number of effects (stages) of the MED-TVC system on the energy and economy of the GT/MED-TVC/RO configuration is explored (Fig. 8). In the combined GT/MED-TVC/RO configuration with capacity 5000 m³/d, the production rates of MED-TVC and RO systems vary according to the number of MED-TVC effects. At effect number of 4, the MED and RO production rates are 2000 m³/d and 3000 m³/d, respectively. It is understood that the more the number of MED/TVC effects, the more the produced fresh water. Hence, at constant production rate of 5000 m³/d, these production rates are changed to 3488 m³/d and 1512 m³/d for the MED and RO, respectively at effect number of 7. It is found that increasing the number of effects from 4 to 7 has no tangible effect on the LCOE. This is due to that at effect number 4, the electricity consumption of desalination systems is 0.65 kWh and by increasing the number of effects from 4 to 7, the electricity consumption decreases from 0.65 kWh to 0.49 kWh and in fact these consumptions are ignorable in comparison to 12 MWh electrical energy generation should be delivered to the users. However, the calculations showed that the rate of change of annul electricity to be generated (AEG) in Eq. (42) and the costs [numerator of Eq. (42)] is such that the LCOE stays unchanged. Also, Fig. 8 shows the effect of number of stages of MED-TVC on the LCOW of GT/MED-TVC/RO configuration. At all effect numbers, the annual water production of both MED-TVC and RO desalination systems is 5000 m³/d, but increasing the number of effects from 4 to 7 leads to the increase of the MED-TVC contribution to 5000 m³/d. Owing to by increasing the production rate of MED-TVC system, increasing rate of the related direct, indirect and other costs of MED-TVC system dominates the decreasing rates of the costs of Ro system in Eq. (25), the numerator of Eq. (43) increases by the number of effects and consequently LCOW increases.

4.4.3. The output temperature and concentration of GT/MED-TVC/RO plant

The output temperature of permeate that is extracted from the GT/MED-TVC/RO unit with MED-TVC and RO water production rates of 2000 m³/d and 3000 m³/d, respectively, was calculated from Eq. (46):

$$M_{MED}h_{MED} + M_{RO}h_{RO} = M_{total}h_{total} \tag{37}$$

where M and h are output ratio and enthalpy of permeate. The results show that the fresh water produced by GT/MED-TVC/RO can be delivered to the users at 31.94°C that is 13.46°C lower than the fresh water temperature that is produced by GT/MED-TVC unit. Also the temperature of fresh water produced by the same GT/MED-TVC/RO with

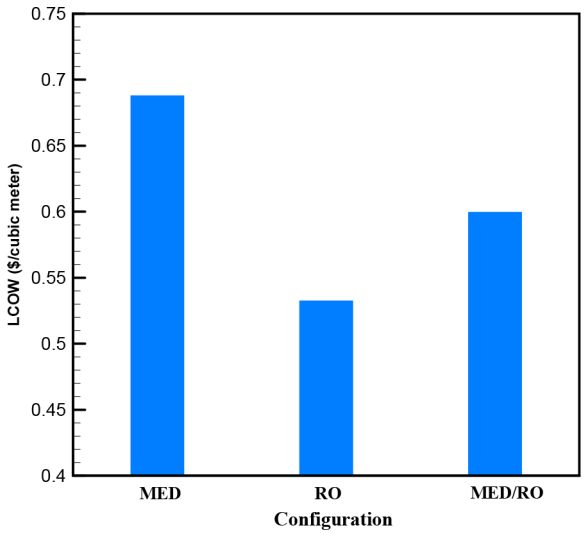

Fig. 7. LCOW for GT/MED-TVC, GT/RO and GT/MED-TVC/RO systems.

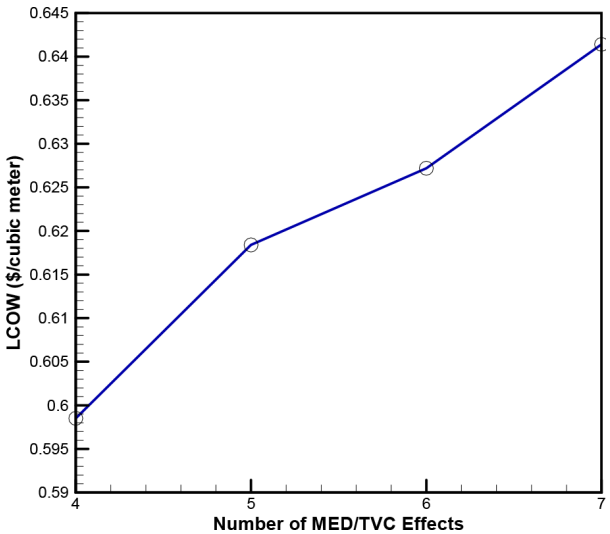

Fig. 8. The effect of number of stages of MED-TVC on the LCOW of GT/MED-TVC/RO system.

7 MED-TVC effects is 37.12°C that is 5.18°C lower than the same GT/MED-TVC/RO with 4 MED/TVC effects.

The output concentration of permeate that is extracted from the GT/MED-TVC/RO unit with MED-TVC and RO water production rates of 2000 m³/d and 3000 m³/d, respectively, was calculated from Eq. (47):

$$M_{MED}X_{MED} + M_{RO}X_{RO} = M_{total}X_{total} \quad (38)$$

where X_{MED} is equal to zero because as mentioned before GT/MED/TVC is salt free. The concentration of freshwater produced by this GT/MED-TVC/RO with 4 MED/TVC effects is 392.6 ppm and with 7 MED/TVC effects is 196.3 ppm.

As can be seen from Fig. 7, the LCOW of GT/MED-TVC/RO is 12.7% higher than that of GT/RO. However, the combined GT/MED-TVC/RO system is more desirable because of the following advantages:

1. The produced fresh water by GT/ME-TVCD/RO configuration has a lower concentration than that by GT/RO for drinking usage.
2. The cost of produced fresh water in GT/ME-TVCD/RO system is lower than the GT/MED-TVC system. Also, the temperature of the fresh water produced by the GT/MED-TVC/RO system is 31.94°C and fresh water produced by the GT/MED system is 45.4°C at MED-TVC effect number 4.

4.4.4. Simple payback time (SPB)

For calculating the simple payback time (SPB) of three dual purpose water/electricity configurations, four scenarios were considered. In scenario A, it was assumed that the revenue of the plant deriving from the electricity production was 0.025 $/kWh and the revenue related to the sale of desalinated water was 0.6 $/m³. The selling unit cost of electricity and water for different scenarios are shown in Table 11.

The effect of applying four defined scenarios (Table 11) on the SPB of three configurations of GT/MED-TVC, GT/RO and GT/MED-TVC/RO are shown in Fig. 9. As shown in Fig. 9, the increase in both revenue of the plant deriving from the electricity production and the revenue related to the sale of desalinated water causes the reduction in the SPB value. According to Eq. (44), because the main investment cost of the GT/RO system is lower than that of two other systems, the Simple Payback Time of the GT/RO has the lowest value for all four Scenarios. As it can be seen from Fig. 9, the difference in the value of SPB in Scenario A for three systems is more than the Scenario D and it can be shown that increasing in electricity and water selling unit costs causes the value of SPB of three defined systems is close to each other. Because the main investment of the GT/MED-TVC/RO system is lower than that of GT/MED-TVC and more than that of GT/RO systems, the SPB of the GT/MED-TVC/RO is in the middle of GT/MED-TVC and GT/RO systems.

Table 11
Unit cost of electricity and water for selling and calculating the plant revenue

Configuration	Electricity and water selling unit costs	
	Electricity ($/kwh)	Water ($/m³)
Scenario A	0.025	0.6
Scenario B	0.035	0.8
Scenario C	0.045	1
Scenario D	0.08	1.1

4.4.5. Sensitivity analysis-fuel cost

Fuel price is one of the parameters that affects unit of cost of the water and electricity. In this part, the LCOE and LCOW were determined under three different fuel price scenarios. Fig.10 shows the LCOE of GT/MED, GT/RO and GT/MED/RO systems for three different fuel prices when the net electricity is generated in the CWP plant and Fig. 11 shows the LCOE of GT/MED, GT/RO and GT/MED/RO systems

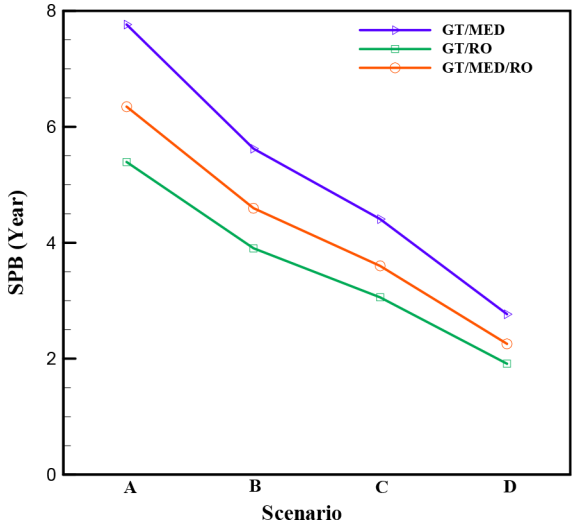

Fig. 9. The effect of four defined scenarios on the SPB in GT/MED-TVC, GT/RO and GT/MED-TVC/RO.

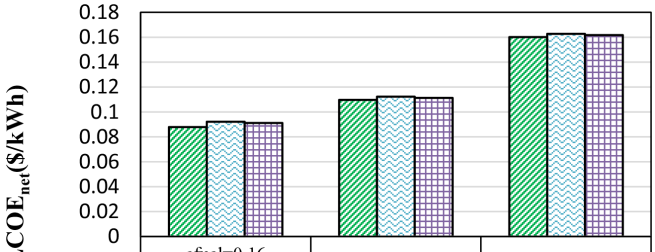

	cfuel=0.16 ($/m3)	cfuel=0.2($/m3)	cfuel=0.3 ($/m3)
GT/MED	0.0879	0.1098	0.1602
GT/RO	0.0922	0.1124	0.1628
GT/MED/RO	0.0912	0.1114	0.1618

Fig. 10. $LCOE_{net}$ for GT/MED-TVC, GT/RO and GT/MED-TVC/RO systems for $c_{fuel} = 0.16\frac{\$}{m^3}$, $c_{fuel} = 0.2\frac{\$}{m^3}$, $c_{fuel} = 0.3\frac{\$}{m^3}$.

for three different fuel prices when the gross electricity is generated in the CWP plant. According to Eq. (42) the LCOE value is related to the fuel cost so as can be seen in Figs. 10 and 11, by increasing the fuel cost, the LCOE is increased. The LCOE of GT/RO is more than that of two other systems for three fuel prices in Fig. 10. In Fig. 10 for net electricity production according to Eq. (42), The denominator of the equation is the same for three systems but as already mentioned the electricity consumption of GT/RO is more than that of two other systems so the annual direct costs for GT/RO is more than that of two other systems. As can be seen in Fig. 11 the LCOE of GT/RO is less than that of two other systems for three fuel prices. According to Eq. (42), AEG for GT/RO is more than that of two other systems because of more gross electricity generation in the GT/RO so the rate of increase in the denominator of the fraction is greater than the numerator.

Fig. 12 shows the LCOW for GT/MED, GT/RO and GT/MED/RO systems for three different fuel prices. According to Eq. (43) the denominator of the fraction is constant for three systems because the fresh water production is constant, As mentioned before, the main investment cost of the GT/MED is more than that of GT/RO system, so the annual direct and indirect cost of the GT/MED is more than that of GT/RO and GT/MED/RO systems, but the electricity consumption of GT/RO is much more than that of GT/MED system that cause the impact of operation costs is more than the other costs such as direct and indirect costs. So, the LCOW of GT/RO is more than that of GT/MED and GT/MED/RO systems.

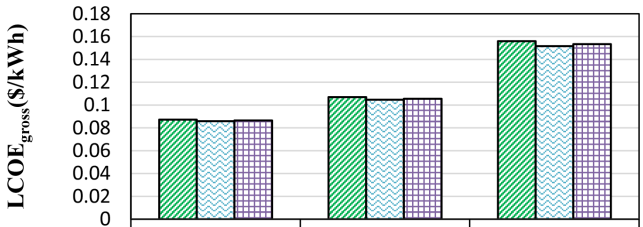

	cfuel=0.16 ($/m3)	cfuel=0.2($/m3)	cfuel=0.3 ($/m3)
GT/MED	0.0873	0.107	0.156
GT/RO	0.0859	0.1047	0.1517
GT/MED/RO	0.0865	0.1056	0.1534

Fig. 11. LCOE$_{gross}$ for GT/MED, GT/RO and GT/MED/RO systems for $c_{fuel} = 0.16\frac{\$}{m^3}$, $c_{fuel} = 0.2\frac{\$}{m^3}$, $c_{fuel} = 0.3\frac{\$}{m^3}$.

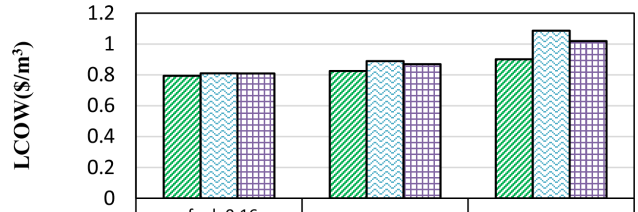

	cfuel=0.16 ($/m3)	cfuel=0.2($/m3)	cfuel=0.3 ($/m3)
GT/MED	0.7949	0.8254	0.9014
GT/RO	0.8108	0.8897	1.087
GT/MED/RO	0.8097	0.8697	1.0198

Fig. 12. LCOW for GT/MED, GT/RO and GT/MED/RO systems for $c_{fuel} = 0.16\frac{\$}{m^3}$, $c_{fuel} = 0.2\frac{\$}{m^3}$, $c_{fuel} = 0.3\frac{\$}{m^3}$.

4.4.6. Sensitivity analysis-MED capital cost

One of the important parameters that affects the LCOW in GT/MED and GT/MED/RO systems is the main investment of MED desalination system. If the main investment of MED system is reduced from 1700 to 1300 ($/m^3/d), in each of the fuel scenarios, the levelized cost of water decreases because according to Eq. (43) all the parameters is constant for each of fuel scenarios, but $C_{CAPEX(D)}$ is greater for MED system with main investment 1700 $/m^3/d. As can be seen from Figs. 13–15 the LCOW of GT/MED/RO is more than that of GT/MED for each MED investment cost because as discussed in section 8.2.2 the electricity consumption of GT/MED/RO is more than that of GT/MED system that cause the impact of operation costs is more than the other costs such as direct and indirect costs. The comparison between two different main investment for each of the fuel scenarios in GT/MED and GT/MED/RO systems have been shown in Figs. 13–15.

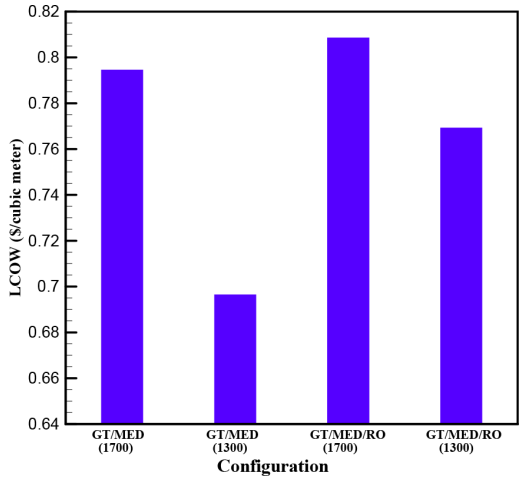

Fig. 13. LCOW for two different main investments in GT/MED and GT/MED/RO systems for $c_{fuel} = 0.16\frac{\$}{m^3}$.

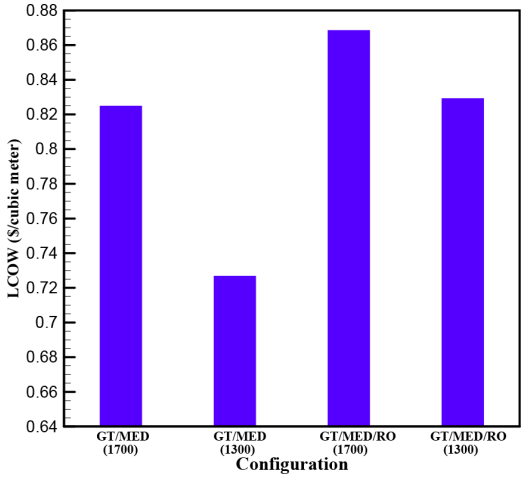

Fig. 14. LCOW for two different main investments in GT/MED and GT/MED/RO systems for $c_{fuel} = 0.2\frac{\$}{m^3}$.

4.5. Effects of plant scale

The results of the previous sections are concerned with a 12 MWh electricity production and 5000 m³/d water production. The larger scales of the CWP plant might decrease the LCOE and LCOW of the system to the lower values. To consider the effect of the scale economy, the LCOE and LCOW of the three different configurations that is discussed earlier delivering the larger capacities using the following well known relationship [12].

$$\frac{Capital\ cost_{L\_scale}}{Capital\ cost_{S\_scale}} = \left(\frac{Capacity_{L\_scale}}{Capacity_{S\_scale}}\right)^{n}$$

where exponent '*n*' was considered to be 0.82. Fig. 16 shows the effect of increasing the scale size of the described configurations on their levelized cost of electricity and Fig. 17 shows the effect of increasing the scale size of the described configurations on their levelized cost of water. As it is obvious from Figs. 16 and 17, for all the three configurations, the increasing of the system scale would considerably decrease the LCOE and LCOW of the systems. As can be seen in Fig. 16 the LCOE of GT/MED system has the lowest value compared with GT/RO and GT/MED/RO systems because the electricity consumption of the MED system (1.5 kWh/m³) is lower than that of the RO system (3.5–4.5 kWh/m³). This figure shows that for larger scales of CHP plant the LCOE of three configurations are close to each other compared with the lower scales for example the difference between LCOE of three configurations for the CHP plant with 120 MWh is about 0.0001 $/kWh. As discussed in section 8.2, because the main investment of the RO is lower than that of by MED system, the unit cost of fresh water by RO is lower than that of by other two configuration so the LCOW of the GT/RO system has the lowest value. As can be seen in Fig. 17, The LCOW of three configurations from scaled ratio 6–10 are almost constant so it is not economical from the aspect of fresh water costs in the three systems.

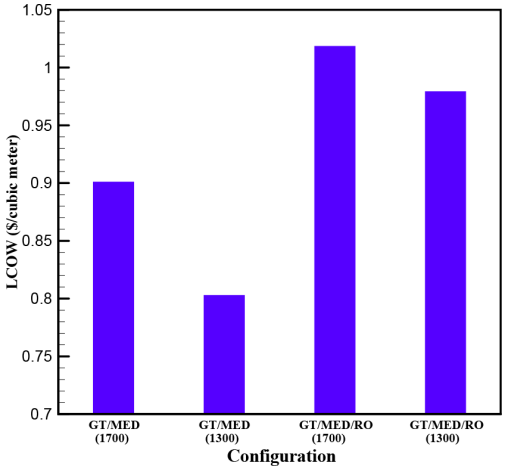

Fig. 15. LCOW for two different main investments in GT/MED and GT/MED/RO systems for $c_{fuel} = 0.3\frac{\$}{m^3}$.

4.6. The portion of fuel cost, direct and indirect costs in LCOW

In this section, it is determined that in each configuration, the fuel cost, the direct and indirect cost of the CWP plant respectively account for the share of the electricity production cost. Also, it is determined that in each configuration, the electricity cost for producing water, the direct and indirect costs of MED and RO and MED/RO plants and the membranes costs respectively account for the share of the freshwater production cost. For 12 MWh plant and 5000 m³/d freshwater production, Figs. 18 and 19 shows the percentage of the discussed costs in each configuration for electricity production and water production costs. As can be seen in Fig. 18, most share of the electricity production cost is dedicated to the fuel cost so the fuel price has a significant impact on the reduction of the levelized cost of

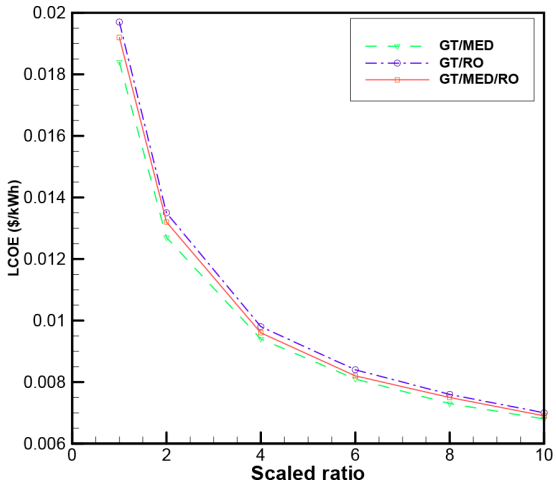

Fig. 16. Effect of increasing of the desalination system scale on the LCOE.

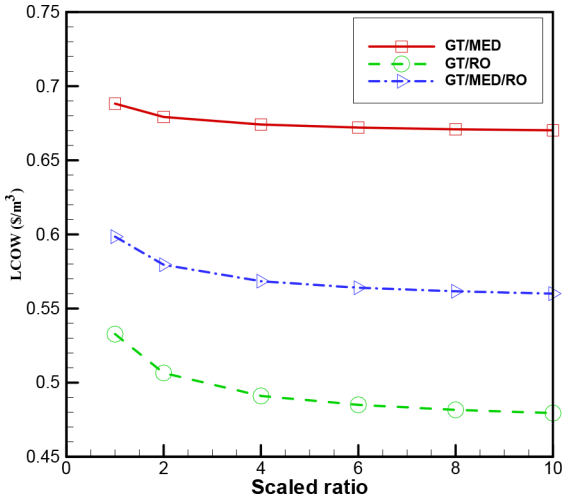

Fig. 17. Effect of increasing of the desalination system scale on the LCOW.

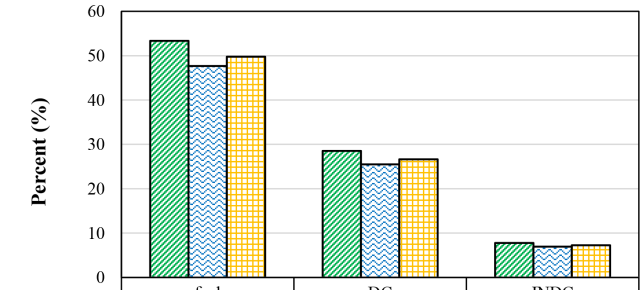

	fuel	DC	INDC
GT/MED	53.35	28.55	7.78
GT/RO	47.69	25.52	6.95
GT/MED/RO	49.79	26.65	7.26

Fig. 18. Percentage of the fuel cost, the direct and indirect cost of CWP plant on LCOE.

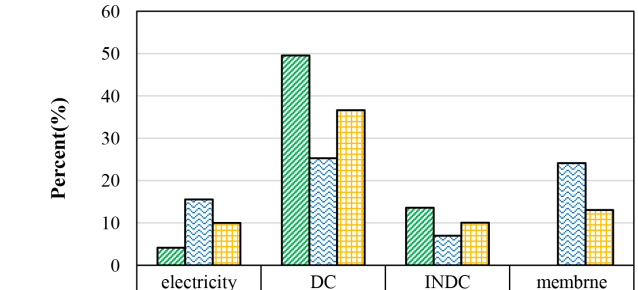

	electricity	DC	INDC	membrne
GT/MED	4.15	49.58	13.59	0
GT/RO	15.55	25.3	6.99	24.13
GT/MED/RO	10.01	36.65	10.07	13.07

Fig. 19. Percentage of the electricity cost, the direct and indirect cost of MED,RO and MED/RO plant and membrane cost on LCOW.

electricity also the unit fuel price for three configurations is assumed to be 0.02 ($\frac{\$}{m^3}$). Fig. 18 shows that between three configurations, the percent of the GT/RO system is lower than the two other configurations due to that the LCOE of the GT/RO system is higher than the GT/MED system.

As Fig. 19 shows, most share of the freshwater production cost is dedicated to the direct cost. The percent of the direct cost for the GT/RO system is lower than the two other systems because the main investment cost for the GT/RO system (900 $/m^3/d) is lower than the main investment cost for the GT/MED system (1700 $/m^3/d). The share of electricity cost for freshwater production in GT/RO system is higher than the GT/MED system because the LCOE of the GT/RO is higher than the GT/MED and also the electricity consumption of the MED system (1.5 kWh/m^3) is lower than that of the RO system (3.5–4.5kWh/m^3).

5. Conclusions

In this research, a comprehensive energy and economic analysis were done for three CWP configurations of GT/MED-TVC, GT/RO and GT/MED-TVC/RO. After mathematical modeling of the individual systems GT, MED-TVC and RO, all these models were validated with the experimental data found in the literature. In was found that increasing the compressor inlet air temperature causes the outlet gas temperature enhancement for both GT/MED-TVC and GT/MED-TVC/RO systems. Also, it was seen that the more the input seawater temperature, the higher the GOR of the MED-TVC system. In the RO energy analysis, the selected membrane was SW30XHR-400i by considering the permeate quality and membrane price. Due to that the electricity consumption of the MED-TVC system is lower than that of the RO system, the of GT/MED-TVC system is the lowest and that of the GT/RO is the highest. Moreover, it was observed that because the main investment cost of RO is lower than that of MED-TVC, the unit cost of fresh water produced by GT/RO and GT/MED-TVC/RO are lower than that of by GT/MED-TVC configuration. Also, if the MED-TVC main investment decreases from 1700 $/m^3/d to 1066 $/m^3/d, the LCOW value for both GT/MED-TVC and GT/RO systems are equal. Moreover, investigating the effect of the MED-TVC stages on the energy and economy of the GT/Med-TVC/RO system revealed that increasing the number of effects from 4 to 7 has no tangible effect on the LCOE. This is due to that the electricity consumption of desalination systems is ignorable in comparison to 12 MWh electrical energy generation should be delivered to the users. Also, it was seen that at constant production rate of 5000 m^3/d, the more the number of MED-TVC effects, the higher the LCOW. Also, mixing the water produced by MED-TVC and RO desalination systems in the GT/MED-TVC/RO configuration led to a drinkable water with desirable concentration and temperature at reasonable cost according to the standards of WHO.

Symbols

A	—	Heat transfer area, m^2
A_f	—	Fin surface area, m^2
A_i	—	Tube inner surface area, m^2
A_o	—	Obstruction area, m^2
A_t	—	Gas side heat transfer surface, m^2
A_w	—	Fluid side heat transfer surface, m^2
AEG	—	Annual electricity generation, (kWh/y)
AF	—	Molar air to fuel ratio
AWP	—	Annual water production, (m^3/y)
B	—	Rejected mass flow rate, (kg/s)
BPE	—	Boiling point elevation, (°C)
C_{CAPEX}(D)	—	Capital annualized direct costs, $
C_{CAPEX}(ID)	—	Capital annualized indirect costs, $
$C_{el(MED)}$	—	MED electricity costs, $
$C_{el(Ro)}$	—	RO electricity costs, $
C_f	—	Fuel costs, $
C_{Ins}	—	Insurance costs, $
C_L	—	Labor costs, $
C_p	—	Specific heat capacity, (kJ/kg°C)
C_{sp}	—	Spare parts replacement costs, $
CR	—	Compression ratio
CRF	—	Capital recovery factor
D	—	Distillated mass flow rate, (kg/s)
CWP	—	Combined water and power
ER	—	Expansion ratio
f	—	Friction coefficient, corrosion coefficient

F — Feed mass flow rate of each effect, (kg/s)
GOR — Gain output ratio
h — Specific enthalpy, (kJ/kg)
i — Annual real interest rate
k_a — Specific heat ratio
k_m — Heat transfer coefficient of tube wall, (kW/kg°C)
LCOE — Levelized cost of electricity, ($/kWh)
LCOW — Levelized cost of water, ($/m^3)
LHV — Low heating value, (J/mol)
$\dot{m}$ — Mass flow rate, (kg/s)
M — Mass flow rate, (kg/s)
M_a — Molar mass of the air, (kg/mol)
M_f — Molar mass of the fuel, (kg/mol)
n — Number of effects, project life time (y), number of mole
NEA — Non equilibrium allowance
N_{memb} — Number of membranes
P — Pressure, kpa
P_{dc} — Discharge pressure, kpa
P_{suc} — Suction pressure, kpa
$\dot{Q}$ — Heat rate, kW
r_{AC} — Compressor pressure ratio
R — Entrainment ratio
R_{el}^a — Revenue related to the sale of electricity, ($/kWh)
R_{fresh} — Revenue related to the sale of desalinated water, ($/m^3)
SPB — Simple payback time, y
T — Temperature, (°C)
T_{app} — Approach point temperature, (°C)
T_{pin} — Pinch point temperature, (°C)
U — Overall heat transfer coefficient, (W/m^2°k)
$\dot{W}_{AC}$ — Compressor work rate, kW
$\dot{W}_{GT}$ — Gas turbine work rate, kW
$\dot{W}_{net}$ — Net work rate, kW
X — Salinity, (ppm)
Y — Percent of theorical air
Z — Cost, $

Greek

η_{AC} — Compressor isentropic efficiency
η_{GT} — Gas turbine isentropic efficiency
λ — Latent heat, (kj/kg)
ΔP_{cc} — Combustion chamber pressure drop, kpa
ΔT_{LMTD} — Logarithmic temperature differences (°C)
ΔT_{min} — Minimum terminal differences (°C)
ΔT_{max} — Maximum terminal differences (°C)

References

[1] H.M. Ettouney, H.T. El-Dessouky, Fundamentals of Salt Water Desalination, 2002.
[2] No Title, (n.d.). http://forsatnet.ir/managers.html.
[3] Z. Gomar, H. Heidary, M. Davoudi, Techno-economics study to select optimum desalination plant for asalouyeh combined cycle power plant in Iran, World Acad. Sci. Eng. Technol. Int. J. Electr. Comput. Energ. Electron. Commun. Eng., 5 (2011) 256–262.
[4] G. Iaquaniello, A. Salladini, A. Mari, A.A. Mabrouk, H.E.S. Fath, Concentrating solar power (CSP) system integrated with MED–RO hybrid desalination, Desalination, 336 (2014) 121–128.
[5] M.H. Khoshgoftar-Manesh, H. Ghalami, M. Amidpour, M.H. Hamedi, Optimal coupling of site utility steam network with MED-RO desalination through total site analysis and exergoeconomic optimization, Desalination, 316 (2013) 42–52.
[6] S. Loutatidou, H.A. Arafat, Techno-economic analysis of MED and RO desalination powered by low-enthalpy geothermal energy, Desalination, 365 (2015) 277–292.
[7] F. Mahbub, M.N.A. Hawlader, A.S. Mujumdar, Combined water and power plant (CWPP)—a novel desalination technology, Desal. Water Treat., 5 (2009) 172–177.
[8] S. Al-Hallaj, F. Alasfour, S. Parekh, S. Amiruddin, J.R. Selman, H. Ghezel-Ayagh, Conceptual design of a novel hybrid fuel cell/desalination system, Desalination, 164 (2004) 19–31.
[9] K. Ansari, H. Sayyaadi, M. Amidpour, A comprehensive approach in optimization of a dual nuclear power and desalination system, Desalination, 269 (2011) 25–34.
[10] S. Sadri, M. Ameri, R.H. Khoshkhoo, Multi-objective optimization of MED-TVC-RO hybrid desalination system based on the irreversibility concept, Desalination, 402 (2017) 97–108.
[11] G. Filippini, M.A. Al-Obaidi, F. Manenti, I.M. Mujtaba, Performance analysis of hybrid system of multi effect distillation and reverse osmosis for seawater desalination via modelling and simulation, Desalination, 448 (2018) 21–35.
[12] M.A. Al-Obaidi, G. Filippini, F. Manenti, I.M. Mujtaba, Cost evaluation and optimisation of hybrid multi effect distillation and reverse osmosis system for seawater desalination, Desalination, 456 (2019) 136–149.
[13] S. Gorjian, B. Ghobadian, Solar desalination: A sustainable solution to water crisis in Iran, Renew. Sustain. Energy Rev., 48 (2015) 571–584.
[14] WHO, Guidelines for drinking-water quality, WHO Chron., 38(4) (2011) 104–108, Edition F.
[15] H. Kurt, Z. Recebli, E. Gedik, Performance analysis of open cycle gas turbines, Int. J. Energy Res., 33 (2009) 285–294.
[16] S. Sanaye, S. Asgari, Analysis and optimization of integrated gas turbine, heat recovery steam generator and multi-effect thermal vapour compression desalination plant, Proc. Inst. Mech. Eng. Part A J. Power Energy, 227 (2013) 919–936.
[17] H. Mokhtari, A. Esmaieli, H. Hajabdollahi, Thermo economic analysis and multi objective optimization of dual pressure combined cycle power plant with supplementary firing, Heat Transf. Res., 45 (2016) 59–84.
[18] V. Ganapathy, Industrial boilers and heat recovery steam generators: Design, Applications, and Calculations, CRC Press, 2002.
[19] M.M. Ashour, Steady state analysis of the Tripoli West LT-HT-MED plant, Desalination, 152 (2003) 191–194.
[20] I.S. Al-Mutaz, I. Wazeer, Development of a steady-state mathematical model for MEE-TVC desalination plants, Desalination, 351 (2014) 9–18.
[21] B. Peñate, L. García-Rodríguez, Current trends and future prospects in the design of seawater reverse osmosis desalination technology, Desalination, 284 (2012) 1–8.
[22] V.G. Gude, Energy consumption and recovery in reverse osmosis, Desal. Water Treat., 36 (2011) 239–260.
[23] M. Meratizaman, S. Monadizadeh, M. Amidpour, Introduction of an efficient small-scale freshwater-power generation cycle (SOFC–GT–MED), simulation, parametric study and economic assessment, Desalination, 351 (2014) 43–58.
[24] V. Fulya, MENA Regional Water Outlook: Part II Desalination Using Renewable Energy, 2011.
[25] H.M. Ettouney, H.T. El-Dessouky, R.S. Faibish, P.J. Gowin, Evaluating the economics of desalination, Chem. Eng. Prog., 98 (2002) 32–39.
[26] B. Najafi, A. Shirazi, M. Aminyavari, F. Rinaldi, R.A. Taylor, Exergetic, economic and environmental analyses and multi-objective optimization of an SOFC-gas turbine hybrid cycle coupled with an MSF desalination system, Desalination, 334 (2014) 46–59.
[27] A. Alzahrani, J. Orfi, Z. Alsuhaibani, Performance analysis of a gas turbine unit combined with MED-TVC and RO desalination systems, Desal. Water Treat., 55 (2015) 3350–3357.

[28] F.N. Alasfour, M.A. Darwish, A.O. Bin Amer, Thermal analysis of ME—TVC+ MEE desalination systems, Desalination, 174 (2005) 39–61.
[29] A. Abbas, On the performance limitation of reverse osmosis water desalination systems, Int. J. Nucl. Desal., 2 (2007) 205–218.
[30] S. Wilson, S.M.R. Fatemi, M.R. Shokri, M. Claereboudt, Status of coral reefs of the Persian/Arabian Gulf and Arabian Sea region, Status of Coral Reefs of the World. 2002, pp. 53–62.
[31] No Title, (n.d.). https://www.seatemperature.org/middle-east/iran/bandar-bshehr-september.htm.
[32] S.A. Avlonitis, M. Pappas, K. Moutesidis, A unified model for the detailed investigation of membrane modules and RO plants performance, Desalination, 203 (2007) 218–228.

Appendix

Seawater thermodynamic properties

A.1. Specific volume

ν is the specific volume of seawater calculated from Eq. (A.1).

$$v_{sw} = \frac{1}{\rho_{sw}} \tag{A1}$$

$$\rho_{sw} = \rho_w + w_s\left(a_1 + a_2T + a_3T^2 + a_4T^3 + a_5w_sT^2\right) \tag{A2}$$

$$\rho_w = 9.999\times10^2 + 2.034\times10^{-2}T - 6.162\times10^{-3}T^2 + 2.261\times10^{-5}T^3 - 4.657\times10^{-8}T^4 \tag{A3}$$

$$a_1 = 8.020\times10^2, a_2 = -2.001, a_3 = 1.677\times10^{-2}, a_4 = -3.060\times10^{-5},\ a_5 = -1.613\times10^{-5} \tag{A4}$$

A.2. Specific entropy

The entropy of seawater that is valid for $10 \le T \le 120$°C, $0 \le W \le 0.12$ kg/kg calculated by (A.6):

$$S_w = 0.1543 + 15.383\times T - 2.996\times10^{-2}\times T^2 + 8.193\times10^{-5}\times T^3 - 1.370\times10^{-7}\times T^4 \tag{A5}$$

$$S_{sw} = S_w - w\begin{pmatrix} c_1 + c_2w + c_3w^2 + c_4w^3 + c_5T + c_6T^2 \\ +c_7T^3 + c_8wT + c_9w^2T + c_{10}wT^2 \end{pmatrix} \tag{A6}$$

$$c_1 = -4.231\times10^2,\ c_2 = 1.463\times10^4,\ c_3 = -9.88\times10^4,\ c_4 = 3.095\times10^5,\ c_5 = 2.562\times10^1,\ c_6 = -1.443\times10^{-1},\ c_7 = 5.879\times10^{-4},\ c_8 = -6.111\times10^1, c_9 = 8.041\times10^1,\ c_{10} = 3.035\times10^{-1} \tag{A7}$$

A.3. Specific enthalpy

The enthalpy of seawater that is valid for $10 \le T \le 120$°C, $0 \le W \le 0.12$ kg/kg calculated by (A.6):

$$h_w = 141.355 + 4202.070\times T - 0.535\times T^2 + 0.004\times T^3 \tag{A8}$$

$$h_{sw} = h_w - w\begin{pmatrix} b_1 + b_2w + b_3w^2 + b_4w^3 + b_5T + b_6T^2 + \\ b_7T^3 + b_8wT + b_9w^2T + b_{10}wT^2 \end{pmatrix} \tag{A9}$$

$$b_1 = -2.348\times10^4, b_2 = 3.152\times10^5, b_3 = 2.803\times10^6,\ b_4 = -1.446\times10^7, b_5 = 7.826\times10^3, b_6 = -4.417\times10^1,\ b_7 = 2.139\times10^{-1}, b_8 = -1.991\times10^4, b_9 = 2.778\times10^4,\ b_{10} = 9.728\times10^1 \tag{A10}$$